Phase behaviour of colloidal assemblies on 2D corrugated substrates

Samir El Shawish[1]**, Emmanuel Trizac**[2] **and Jure Dobnikar**[3,4]

[1] Reactor Engineering Division, Jožef Stefan Institute, Jamova 39, 1000 Ljubljana, Slovenia
[2] Laboratoire de Physique Théorique et Modèles Statistiques (CNRS UMR 8626), Université Paris-Sud, 91405 Orsay Cedex, France
[3] Department of Theoretical Physics, Jožef Stefan Institute, Jamova 39, 1000 Ljubljana, Slovenia
[4] Department of Chemistry, University of Cambridge, Lensfield Road, Cambridge, CB2 1EW, UK

E-mail: trizac@lptms.u-psud.fr and jd489@cam.ac.uk

Abstract
We investigate—using Monte Carlo computer simulations—the phase behaviour of dimeric colloidal molecules on periodic substrates with square symmetry. The molecules are formed in a two-dimensional suspension of like charged colloids subject to periodic external confinement, which can be experimentally realized by optical methods. We study the evolution of positional and orientational order by varying the temperature across the melting transition. We propose and evaluate appropriate order parameters as well as the specific heat capacity and show that the decay of positional correlations belongs to a class of crossover transitions while the orientational melting is a second-order phase transition.

S Online supplementary data available from stacks.iop.org/JPhysCM/24/284118/mmedia

(Some figures may appear in colour only in the online journal)

1. Introduction

Understanding, creating and controlling patterned structures on nano- and microscales is an important objective of modern materials science [1]. Studying colloidal ordering at surfaces provides valuable insights into the underlying mechanisms. Complex surfaces with submicron periodicities can direct self-assembly of highly oriented responsive colloidal crystals [2] and biologically active substrates [3, 4]. Charged objects are ubiquitous in the colloidal domain and electrostatic interactions have been widely employed in colloidal assembly. Predominantly spherical colloidal particles have been studied, while comparatively little work has been devoted to the behaviour of anisotropic charged composite objects in a solution. The spherical shape is, however, more of an exception than a rule in the colloidal realm, and from a fundamental point of view, understanding the mechanisms directing the assembly of anisotropic charged colloids is at least equally important. Moreover, it enables the design of novel ordered micro- and nanostructures.

Experimentally, patterned substrates are typically created by either optical manipulation [5] or surface deposition [6, 7]. Multiple charged spherical colloids can then be confined within the traps. If the number of colloids N is an integer of the number of traps N_{tr}, at strong enough confinement, monodisperse clusters or 'colloidal molecules' (in general anisotropic, at least for small n) constituted of $n = N/N_{tr}$ colloids are confined to each of the traps. The coupling between the anisotropy of the charged 'molecules' and screening by microions in the solution is surprisingly nontrivial [12, 14, 15]. The multipole moments generated by the molecular anisotropy are all screened in a similar fashion, so that inter-molecular interactions feature nontrivial angular dependence affecting the symmetry of the ordering in a subtle way. Therefore, where large-enough electrostatic interactions take place, orientationally ordered 'colloidal molecular crystals' are formed. Crystals with a remarkably rich variety of orientational ordering have been observed [8–17]. In the case of like charged repulsive colloids the molecular size is determined by the interplay between the electrostatic repulsion and the confinement forces, while

the inter-molecular electrostatic interactions determine the type of rotational ordering of the molecules. The ground state behaviour of such colloidal molecular crystals has been explored in several studies [12–15, 17], however, in order to assess their thermal stability the complete phase behaviour needs to be explored. Molecular dynamics simulations [10] have been performed showing the generic phase behaviour of colloidal molecular crystals ($n = 2$–4) on square and triangular periodic substrates. A two-stage melting has been reported where first the orientational and then the positional order vanishes. Similarly, in an experiment [8, 9] laser induced freezing and melting has been observed: upon increasing the confinement strength colloidal trimers confined to a triangular lattice went through a transition from liquid to crystal and back to modulated liquid. Here, we focused on colloidal dimers ($n = 2$) on two-dimensional square periodic substrates and performed parallel tempering Monte Carlo simulations to study the melting process in detail. We defined appropriate order parameters describing the two-stage melting and characterized the order–disorder transition for both the orientational and positional correlations. It was found that the orientational melting is a second-order phase transition diverging specific heat at the transition temperature, while the decay of the positional order is not a phase transition but rather a gradual crossover-type transition.

2. Model and methods

We consider a system of like charged spherical colloids confined to a plane and immersed in a suspension of monovalent counterions and salt ions (the solvent is hereafter considered as a structure-less medium of constant dielectric permittivity). The microions neutralize the total charge and mediate repulsive screened Coulomb interactions among the colloids. We assume the pairwise additive Yukawa potentials, and do not consider many-body contributions to the electrostatic interactions because the geometry of the problem and the typical screening parameters explored are in the regime where pairwise additivity is an excellent assumption [18]. The colloids are subject to additional periodic external confinement, introduced by laser tweezers [8, 10] creating a set of potential traps for the colloids. The number of traps $N_{tr} = N/2$ introduced by the confinement is exactly half of the number of colloids. The total interaction energy in the dimensionless form is:

$$E = \sum_{i=1}^{N} \sum_{j \neq i}^{N} \frac{e^{-\kappa r_{ij}}}{r_{ij}/l} - A \sum_{i=1}^{N} \cos(2\pi x_i/l) + \cos(2\pi y_i/l), \quad (1)$$

where (x_i, y_i) are the Cartesian coordinates of colloid i in the plane, r_{ij} the distance between colloids i and j and $1/\kappa$ is the Debye screening length. The unit of length l is the inter-trap distance (see figure 1), and the parameter A is a measure of the relative strength of the confinement over the electrostatic forces. The physical parameters governing the phase behaviour of the system are κl, A and the temperature T. At low temperatures and strong confinement each trap is occupied by exactly
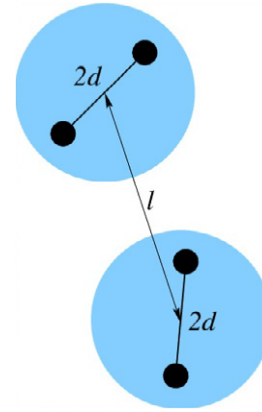

Figure 1. Schematic representation of colloidal dimers in potential traps. The distance between the centres of the potential traps l is the unit of length. In a strong enough confinement, exactly two colloids occupy each trap forming a colloidal dimer with a characteristic size $2d$. The colloidal 'molecules' are well defined, when $2d \ll l$.

two colloids forming an elongated colloidal dimer. Due to the dimer–dimer electrostatic interactions, the dimers order into orientationally ordered colloidal molecular crystals. On raising the temperature, the orientational order of the dimers decays and eventually it becomes possible for single colloids to hop between the traps, thus destroying the dimers and forming a modulated liquid state.
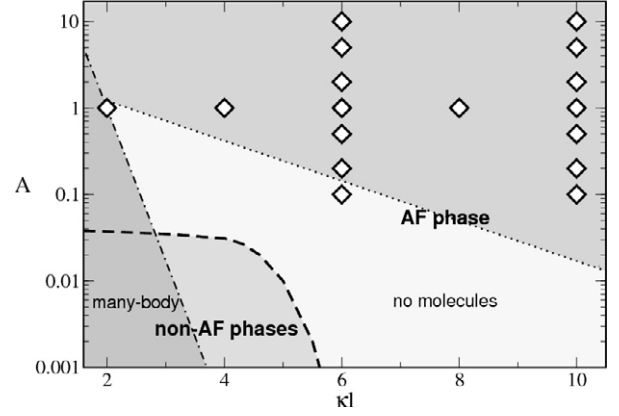
We used parallel tempering Monte Carlo (PTMC) simulations to simulate M replicas of the system, each in the canonical ensemble, at temperatures T_i ranging from $T_1 = 10^{-4}$ to $T_M = 1$ allowing for configurational swaps between systems with adjacent temperatures [19] (we chose a geometric temperature profile, thus $T_i/T_{i+1} = $ const). Apart from single colloid moves and configurational swaps we also implemented dimer rotations that became important at low temperatures. The colloids are treated as point-like charges and the periodic boundary conditions are applied to the simulation box.

In figure 2 we show the energy histograms $P(E)$ for our model system at the lowest five temperatures and three system sizes. Overlap of $P(E)$ between adjacent replicas, at different temperatures, allows for acceptance of the configuration swaps; in our simulations the target replica exchange probability is set to 0.2 (empirically, we found that values around 0.2 are optimal). To achieve this, for a given number of colloids N, the number of replicas M is chosen as $M = \sqrt{50N}$. We have studied systems with $(N, M) = (8, 20)$, $(32, 40)$, $(72, 60)$, $(128, 80)$ and $(200, 100)$. From the upper inset in figure 2 we see that the width of $P(E)$ (which is proportional to the standard deviation σ_E of the distribution) decreases as $1/\sqrt{N}$ so that the number of replicas M should indeed scale as $\sqrt{N}$ to maintain a constant overlap. We note that T_i (except T_1 and T_M) have different values for different system sizes N. We first examined the ground state phase diagram of dimers ($n = 2$) on a square lattice by PTMC simulations. The parameter space (κl, A) we have explored is depicted in figure 3 where several regions are highlighted. In most of the parameter space on
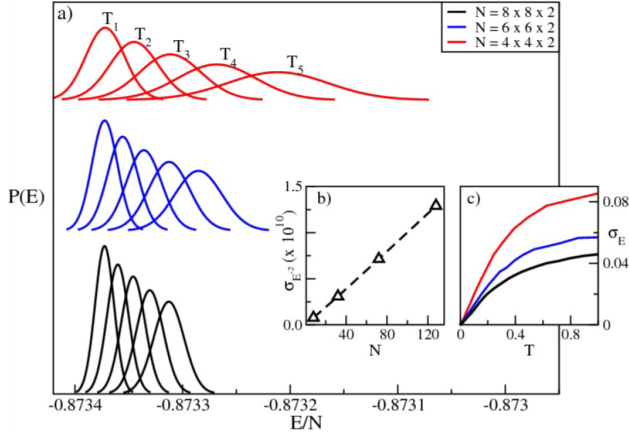
Figure 2. (a) Energy histograms (Gaussian distributions) $P(E)$ calculated at five lowest temperatures T_1–T_5 in equilibrated PTMC simulations for three system sizes $N = 32, 72, 128$ (shifted for clarity). The values of the physical parameters are $\kappa l = 10$ and $A = 0.6$. Insets: standard deviation σ_E of the distributions $P(E)$ as a function of (b) the number of colloids N at the lowest temperature $T = T_1$ and (c) the temperature T at the values of N displayed in the main plot.


Figure 3. $T = 0$ phase diagram of dimers on a square lattice of traps. The line separating the AF region from the non-AF region is schematic and was calculated on a $N = 32$ system using PTMC method. The diamond symbols are placed at the positions in the parameter space where the finite temperature behaviour has been explored. The regions of the parameter space where many-body interactions are dominant and where the molecules are not well defined are marked with shades of grey. Note that the phase diagram where cosine confinement is replaced by the parabolic trapping [14] is considerably richer.

the figure (right-hand side) the ground state configuration of the colloids is antiferro-like (AF), meaning that the dimers' directions in neighbouring traps are perpendicular. Structures different from AF are observed at low A and κl. Typically, at vanishing confinement strength A, the colloids arrange into a hexagonal lattice and upon increasing A, the structure evolves via I-phases (chequerboard arrangement with neighbouring dimers' relative angles less than $\pi/2$, see [14, 12]) into an AF arrangement (where the angle between neighbouring dimers is $\pi/2$). At low values of the screening parameter κl, the electric double layers are of comparable size to the lattice spacing and many-body effects among colloids are likely to play an important role in orientational ordering. We have roughly estimated and highlighted the many-body dominated region with dark grey shading in figure 3. Most of the non-AF phases we discussed above (including those reported in the literature [10] where the parameters were $\kappa l = 2$ and $0 < A < 0.64$) are in or close to this region, which means that their stability would need to be re-assessed by applying the many-body Poisson–Boltzmann theory. The behaviour in this regime is interesting; however it is experimentally difficult to access and so was not the focus of our present study. We would also like to stress that in a large part of the parameter space where the confinement is relatively weak, the size of the 'molecules' in the traps is significant with respect to the lattice spacing and the notion of the molecule becomes obscure. We have provisionally marked this region with a light grey shading (please note that there is a certain degree of arbitrariness in defining the boundaries of such regions). To study the phase behaviour, we concentrated on the remaining part of the parameter space, where molecules are well defined and many-body effects are negligible. Such a regime is also where most of the experimental studies [8, 9] have been performed. In this parameter regime the ground state at $T = 0$ is at the AF phase. We have analysed the phase behaviour as

a function of temperature at the points described by three sets of parameters (depicted by the diamond symbols in figure 3): $0.1 \le A \le 10$, $\kappa l = 10, 6$ and $A = 1$, $2 \le \kappa l \le 10$.

3. Results

In figure 4 we show typical snapshot configurations at different temperatures across the melting transition. The rightmost column shows the energy and moments of positional and angular distributions as a function of temperature. In the snapshots, one can observe AF configurations with long-range positional and orientational order, positionally ordered (exactly two colloids per trap) but orientationally disordered states and liquid-like disordered configurations. In order to quantify the positional order, we show normalized distributions of the trap occupancy $P(N_t)$, which is narrow and peaked at $N_t = 2$ at low enough temperatures, while it broadens around the average $N_t = 2$ at higher temperatures. From these distributions it seems natural to extract a T-dependent order parameter as $P(2)$, measuring the ratio of traps in the system with exactly two colloids. Any deviations from the saturated value $P(2) = 1$ signal the presence of positional melting. A smooth decrease of $P(2)$ with increasing T is a sign of a crossover transition rather than a phase transition; this is supported by the lack of symmetry breaking at the transition. In this respect, a crossover transition temperature T_{c1} cannot be rigorously defined, yet we decide to mark with T_{c1} the beginning of the crossover at the point where $P(2)$ starts to deviate from 1. At that temperature on average the $N_{tr} - 2$ traps still host exactly two colloids, while two of the traps exchange one colloid to host one and three colloids. The threshold value of the order parameter is $P(2) = 1 - 2/N_{tr}$. From the results at $\kappa l = 10$ and $A = 0.6$ we estimate
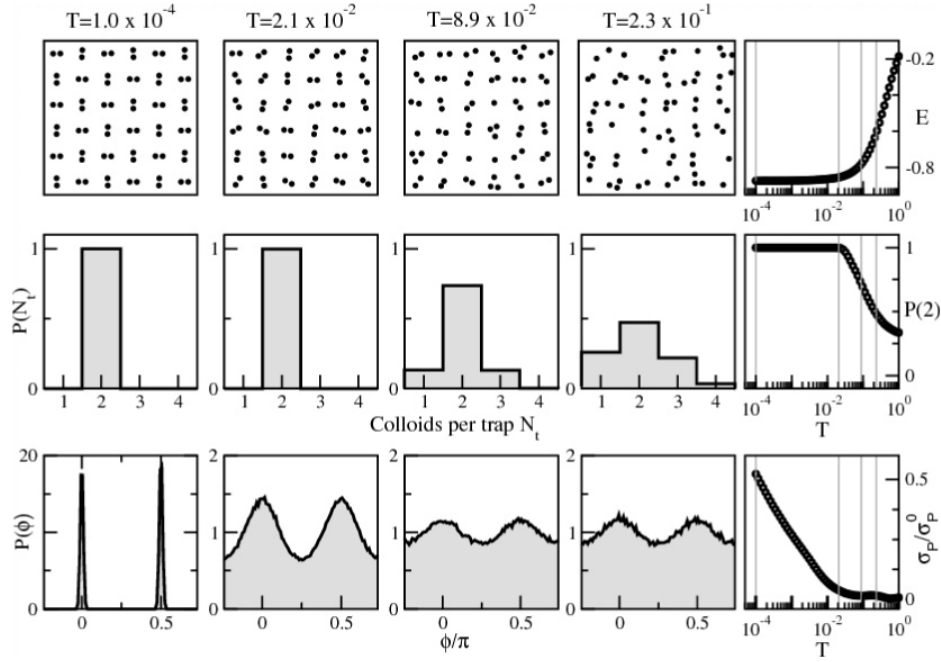
Figure 4. Results of the PTMC simulations of 72 colloids subject to a periodic array of 36 traps at $\kappa l = 10$ and $A = 0.6$. Top row: typical colloidal configurations from the simulations at four selected temperatures. The right column shows the energy $E(T)$ versus temperature T (the four vertical lines denote the temperatures of the configurations on the left). Mid-row: distribution of the number of colloids per traps for the same parameters as in the top row. The right column shows the proportion of double-occupied traps $P(2)$ as a function of temperature T. Bottom row: angle distributions $P(\phi)$ of dimers (or higher n-mers if there are more than two colloids per trap (see footnote 5)) calculated at the same four temperatures as above. The right column shows the temperature dependence of the spreading parameter as a measure of angular anisotropy.

$T_{c1} \approx 2 \times 10^{-2}$. The so-defined quantity is showing negligible finite size effects. At low temperatures the colloidal dimers are orientationally correlated. This is indirectly demonstrated in the bottom row of figure 4 where the angle distributions $P(\phi)$ of dimers at various temperatures[5] are depicted. At the lowest temperature, two narrow peaks of equal height imply that half of the dimers lie horizontally ($\phi = 0$) and the other half vertically ($\phi = \pi/2$), as expected for the AF phase. To characterize the above distributions with a meaningful scalar measure, we define the spread σ_p of the distribution $P(\phi)$: $\sigma_P^2 = 1/N_{\text{bin}} \sum_i (P_i - 1)^2$, where N_{bin} is the number of bins used to sample the variable ϕ. In order to have a quantity bounded by 1, we define the spreading parameter σ_P/σ_P^0, where $\sigma_P^0 = \sqrt{N_{\text{bin}}/2 - 1}$ is the zero temperature limit of σ_P in the AF phase. At large T the value of σ_P/σ_P^0 is zero, indicating an orientationally disordered configuration and it starts increasing upon lowering the temperature below T_{c1}. However, the spreading parameter is not a suitable order parameter for studying the details of the orientational melting transition, since it only deals with one-dimer statistics and therefore does not capture dimer–dimer angular correlations.

To properly account for the angular correlations in dimeric coverings, we define a new order parameter analogue to the Fourier transform of the spin–spin correlator[6]. We start from the averaged static correlation function that measures average angle–angle correlation between two traps separated by $\boldsymbol{\delta}$

$$O(\boldsymbol{\delta}) = \frac{1}{N_{\text{tr}}} \sum_{i=1}^{N_{\text{tr}}} \langle |\cos(\phi_{i+\boldsymbol{\delta}} - \phi_i)| \rangle \tag{2}$$

where N_{tr} denotes the number of traps in a system and ϕ_i measures the orientation of the dimer in the ith trap and $\langle \cdots \rangle$ denotes thermal averaging. Since dimers are not directed and therefore ϕ and $\phi \pm \pi$ indicate the same orientation, we use the absolute value in equation (2). The function $O(\boldsymbol{\delta})$ is bounded on $[0, 1]$; in order to compute its Fourier transform, we first expand its range to $[-1, 1]$ by transforming it: $O(\boldsymbol{\delta}) \to 2O(\boldsymbol{\delta}) - 1$. The Fourier transform then reads:

$$O(\mathbf{q}) = \frac{1}{N_{\text{tr}}} \sum_{\boldsymbol{\delta}} (2O(\boldsymbol{\delta}) - 1) e^{i\mathbf{q} \cdot \boldsymbol{\delta}} \tag{3}$$

$\mathbf{q}$ being a 2D ordering wavevector. The temperature variation of $O(\mathbf{q})$ across the melting transition from AF to modulated liquid is depicted in figure 5. In an ideally ordered AF phase at $T = 0$, characterized by modulation $\mathbf{q} = \mathbf{q_0}$, the order parameter saturates, $O(\mathbf{q_0} = (\pi, \pi)) = 1$. At high

---

[5] An n-mer orientation is defined as an angle ϕ between the horizontal axis and n-mers's principal axis with the smallest principal moment. Principal axes and principal moments are obtained by diagonalizing the 2×2 area moment of inertia tensor $J_{ij} = \int (r^2 \delta_{ij} - r_i r_j) \, \mathrm{d}A$ where $i, j = x, y$ and distance r_i is measured relatively to the centre of mass. Since colloids are viewed as point-like objects, the area integral in J_{ij} is further reduced to a sum over all colloid positions within a given n-mer. This definition of orientation is robust for all $n > 1$ and all shapes.

[6] In spin systems, the spin–spin correlation function $\Gamma(\boldsymbol{\delta}) = 1/N \sum_i \mathbf{S}_{i+\boldsymbol{\delta}} \cdot \mathbf{S}_i$, where spins $\mathbf{S}_i$ are axial vectors, translates to $\Gamma(\boldsymbol{\delta}) = 1/N \sum_i \cos(\phi_{i+\boldsymbol{\delta}} - \phi_i)$ for $|\mathbf{S}_i| = 1$.
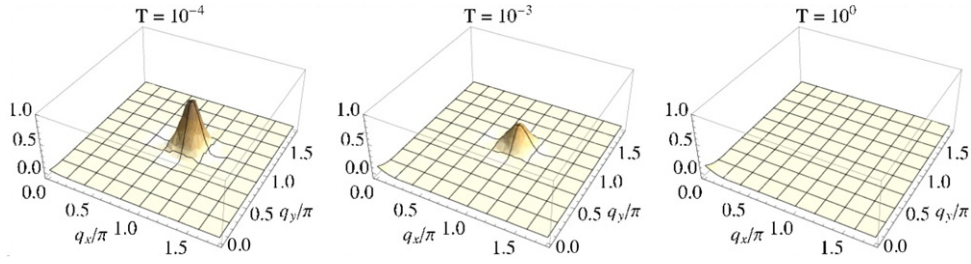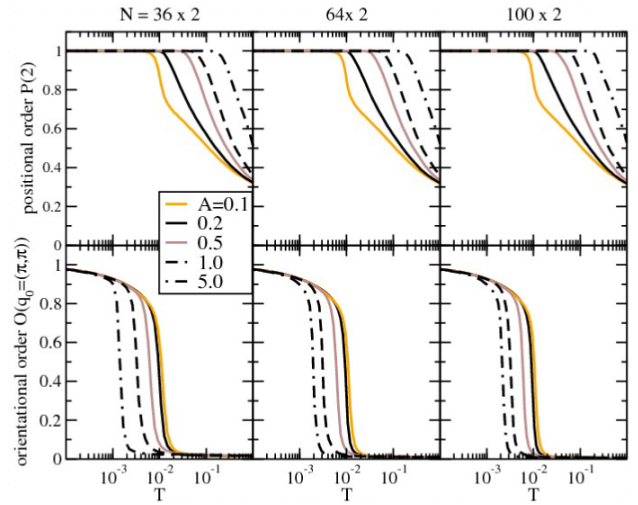
Figure 5. The orientational order parameter $O(\mathbf{q})$ as a function of the two-dimensional wavevector $\mathbf{q}$ at three temperatures across the melting transition ($\kappa l = 10$, $A = 1$). At the lowest temperature (AF phase) the peak $O(\mathbf{q_0} = (\pi, \pi))$ reflects the modulation of the angular orientation of the dimers. Upon raising the temperature, this peak gradually decays and at high temperature (modulated liquid phase), where the dimers are uncorrelated, a peak at $\mathbf{q} = \mathbf{0}$ emerges.
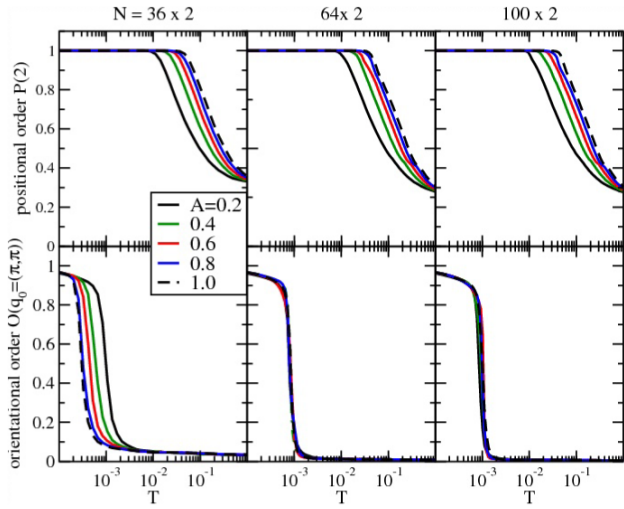
Figure 6. Melting transitions of AF phase for $\kappa l = 10$ and various trap strengths $A = 0.2$–1 and three system sizes. Upper row: the positional order parameter $P(2)$ as a function of T. Lower row: the temperature dependence of the orientational order parameter $O(\mathbf{q_0} = (\pi, \pi))$ defined in equation (3).

Figure 7. Same as figure 6 for $\kappa l = 6$ and trap strengths A from 0.1 to 5.

temperatures, in contrast, any pair of traps is uncorrelated, which gives a vanishing $O(\mathbf{q})$ for all non-zero wavevectors: $O(\mathbf{q} \neq \mathbf{0}) \propto 1/N_{\mathrm{tr}}$.[7] In figure 6 we compare the orientational and positional order–disorder transitions at $\kappa l = 10$ for several confinement strengths A at three system sizes. In the upper row we plot the maximum value of the trap occupancy distribution $P(2)$ as an order parameter for the positional order. We see that the melting transition is gradual, depends on the confinement strength and shows very little size dependence. In the lower row we show the temperature dependence of the orientational order parameter $O(\mathbf{q_0})$ (equation (3)) using the antiferro-ordering wavevector $\mathbf{q_0} = (\pi, \pi)$. It varies from 1 (AF phase) at low temperatures to 0 (orientational disorder) at high T. In contrast to the positional

melting, the transition is now sharp and grows sharper with increasing system size. This behaviour is a signature of a second-order phase transition with diverging correlation length. We also note that at the transition the system reduces translational symmetry with respect to the periodicity of the underlying trap potential. In figure 7, the same quantities are plotted for $\kappa l = 6$. Very similar results have been obtained at all other parameter values κl and A marked on figure 3 (results not shown). We therefore conclude that there are—in agreement with previous results [10]—two transitions going on in the system upon cooling from the liquid phase. At $T_{c1} \approx 10^{-2}$ a gradual crossover ordering transition to the positionally ordered structures sets in, and at $T_{c2} \approx 10^{-3}$ a second-order phase transition from orientationally disordered to ordered state. In order to further strengthen the evidence for a second-order phase transition, we have also calculated the specific heat as a function of temperature. The specific heat of a finite canonical system is given by the energy fluctuations:

$$C = \frac{\langle E^2 \rangle - \langle E \rangle^2}{T^2}. \tag{4}$$

We have evaluated this expression and observed a narrow peak in C at T_{c2} showing the expected system size dependence for a second-order phase transition (in an infinite system the

---

[7] At $T \to \infty$, where the correlations between traps are nonexisting, according to the definitions in equation (2), $O(\boldsymbol{\delta} = \mathbf{0}) \equiv 1$ and $O(\boldsymbol{\delta} \neq \mathbf{0}) \equiv 2/\pi$. Consequently, from equation (3), it follows that $O(\mathbf{q} = \mathbf{0}) = 4/\pi - 1 + (2 - 4/\pi)/N_{\mathrm{tr}}$ and $O(\mathbf{q} \neq \mathbf{0}) = (2 - 4/\pi)/N_{\mathrm{tr}}$. The wavevector $\mathbf{q} = \mathbf{0}$ is special in that it leads to a finite value $O(\mathbf{0})$ even for infinite systems $N_{\mathrm{tr}} \to \infty$. In figure 5 at high temperature ($T = 1$) we observe the peak at $\mathbf{q} = \mathbf{0}$, while the values for any other wavevector are $O(\mathbf{q} \neq \mathbf{0}) = (2 - 4/\pi)/N_{\mathrm{tr}}$, which decays to zero with the system size.
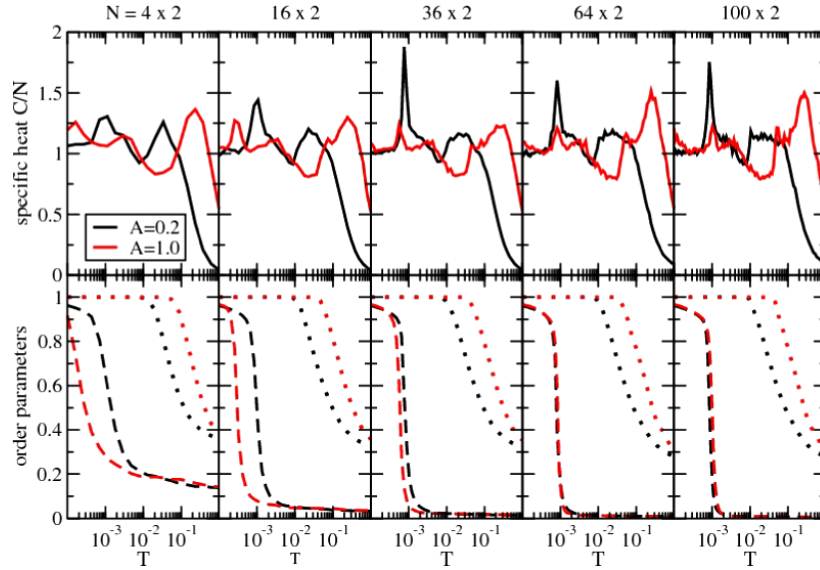
Figure 8. Upper row: temperature dependence and finite size scaling of the specific heat per colloid C/N at $\kappa l = 10$ and two values of A. Lower row: the corresponding variation of the orientational $O(\mathbf{q_0})$ (dashed lines) and positional $P(2)$ (dotted lines) order parameters.

specific heat would diverge at T_{c2}). In contrast, there is a broad size-independent peak positioned at T_{c1}. In figure 8, we present the specific heat curves as a function of temperature and system size at two extreme values of A demonstrating that a maximum increase of both order parameters coincides with peak positions in specific heat function. An interesting observation is that the position of the crossover transition T_{c1} shifts towards higher temperatures with increasing trap strength A, while the position of the phase transition T_{c2} shows a weaker dependence on A. From analysing the finite size scaling (see the supplementary material available at stacks. iop.org/JPhysCM/24/284118/mmedia) of the two transition temperatures we conclude that both T_{c1} and T_{c2} are finite in the thermodynamic limit[8].

4. Discussion

To summarize, we present (figure 9) phase diagrams showing both transition temperatures versus κl at fixed confinement strength and versus A at fixed κl. The crossover transition T_{c1} has been somewhat arbitrarily defined as the temperature at which the positional melting starts and the value of the order parameter $P(2)$ drops from 1 to $1 - 2/N_{tr}$. On the other hand, T_{c2} was extracted as the point of the steepest decrease of the orientational order parameter $O(\mathbf{q_0})$, exactly matching the position of the diverging peak in the specific

heat C (figure 8). With increasing screening strength κl, both critical temperatures decrease (see left panel in figure 9). This is due to weaker inter-trap interactions that directly control orientational ordering (T_{c2}) and also to trapping forces and average distances between the dimers, which affects positional ordering (T_{c1}). Increasing A has a similar effect on T_{c2} (see middle and right panels in figure 9) since larger A means smaller dimers and hence weaker inter-trap forces. However, positional order is of course stronger at larger A, therefore higher temperatures are needed to destroy it. At large enough values of κl and A we observe the two-stage melting with the phase transition from ordered solid to partially ordered solid (without orientational order) and the crossover melting of the positional order from partially ordered solid to modulated liquid. Interestingly, at longer screening lengths (smaller κl) and weaker confinement the crossover transition disappears and the ordered solid melts directly into a modulated liquid via a second-order phase transition. This can also be observed in figure 7 (first row, orange line with $A = 0.1$) where the $P(2)$ curve exhibits a sudden change in the slope, precisely at T_{c2}. The phase diagram reported here is qualitatively consistent with the result of the Langevin simulations reported in [10]. The screening lengths considered in our work ($\kappa l = 6, 10$) are much shorter than in [10] ($\kappa l = 2$), therefore the phase diagrams in figure 9 are shifted to lower values of the confinement A as compared to figure 4 in [10]. In [13] spin models were constructed to analytically describe orientational ordering of colloidal molecules on periodic lattices. Remarkably, their analytically obtained orientational melting transition for trimers on triangular lattice coincides with the corresponding transition for dimers on square lattices in [10]. Crystalline structures of dimers on triangular lattice were also examined in [13] showing interesting transitions between herringbone, ferromagnetic, 'Japanese 6 in 1', paramagnetic and antiferromagnetic ordering. However, several approximations had to be made

---

[8] We have looked at the critical behaviour and evaluated the critical exponents for the phase transition at T_{c2}. The specific heat scales as $C \propto |T - T_{c2}|^\alpha$. The estimate from the available system sizes is $\alpha \approx 1/6$. Larger system sizes would have to be considered in order to obtain the exponent more accurately. The obtained value lies in between the spin model values for the Ising model ($\alpha = 0$) and the three-state Potts model ($\alpha = 1/3$) [20]. The corresponding exponent for the order parameter $O(\mathbf{q_0})$ proved to be more difficult to assess by finite size scaling. Roughly, the value seems to be $\beta \approx 0.2$ in contrast to the spin model values (Ising: 1/8 and three-state Potts: 1/9). The more elaborate evaluation of the critical exponents is out of the scope of the present paper.
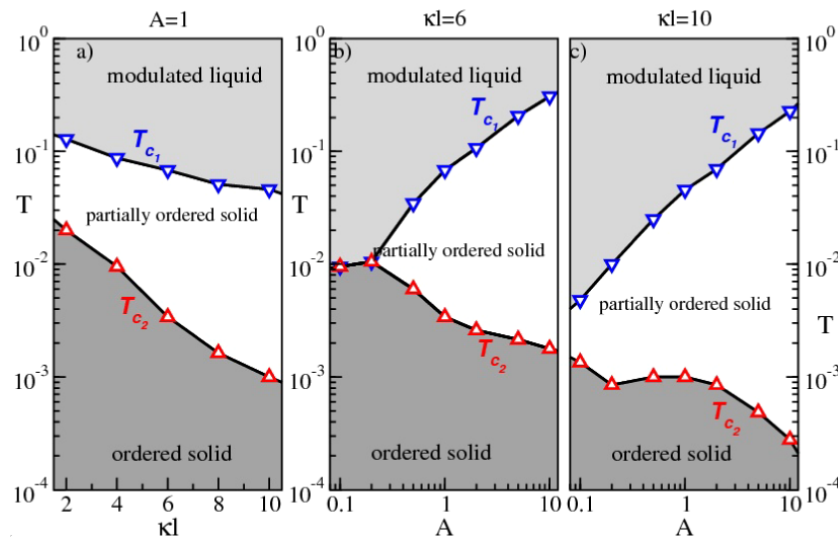
Figure 9. Phase behaviour of dimers on the square lattice as calculated in the largest system with $N = 200$ colloids: (a) transition temperatures versus κl at fixed confinement strength $A = 1$; (b) transition temperatures versus A at fixed screening $\kappa l = 6$ and (c) $\kappa l = 10$.

in order to reduce the colloidal system to a Potts-like model; they assumed rigid dimers placed on the lattice points were interacting only with their nearest neighbours and so were restricted to discrete orientations compatible with the lattice symmetry. In [14] we have already discussed that the discrete angle approximation does not apply to the experimental system of colloids trapped by laser tweezers. Further to that, while the nearest-neighbour approximation seems well justified for triangular lattices, it is qualitatively wrong on square substrates [14]; therefore it seems difficult to extend the conclusions of [13] to colloidal systems and to square-like patterned substrates.

Acknowledgments

References

[1] Alivisatos A P, Johnsson K P, Peng X, Wilson T E, Loweth C J, Bruchez M P Jr and Schultz P G 1996 *Nature* **382** 609
[2] Lin K, Crocker J C, Prasad V, Schofield A, Weitz D A, Lubenski T C and Yodh A G 2000 *Phys. Rev. Lett.* **85** 1770
[3] Barrya E and Dogic Z 2010 *Proc. Natl Acad. Sci.* **107** 10348
[4] Falconnet D, Koenig A, Assi F and Textor M 2004 *Adv. Funct. Mater.* **14** 749
[5] Hoogenboom J P, Vossen D L J, Faivre-Moskalenko C, Dogterom M and van Blaaderen A 2002 *Appl. Phys. Lett.* **80** 4828
[6] Yin Y, Lu Y, Gates B and Xia Y 2001 *J. Am. Chem. Soc.* **123** 8718
[7] Karakurt I, Leiderer P and Boneberg J 2006 *Langmuir* **22** 2415
[8] Brunner M, Bechinger C and Leiderer P 2001 *Phys. Rev. Lett.* **86** 930
[9] Brunner M and Bechinger C 2002 *Phys. Rev. Lett.* **88** 248302
[10] Reichhardt C and Olson C J 2002 *Phys. Rev. Lett.* **88** 248301
[11] Reichhardt C and Olson-Reichhardt C J 2005 *Phys. Rev. E* **71** 062403
[12] Agra R, van Wijland F and Trizac E 2004 *Phys. Rev. Lett.* **93** 018304
[13] Šarlah A, Franosch T and Frey E 2005 *Phys. Rev. Lett.* **95** 088302
Šarlah A, Frey E and Franosch T 2007 *Phys. Rev. E* **75** 021402
[14] El Shawish S, Dobnikar J and Trizac E 2008 *Soft Matter* **4** 1491
[15] Trizac E, El Shawish S and Dobnikar J 2010 *An. Acad. Bras. Cienc.* **82** 87
[16] Reichhardt C and Olson Reichhardt C J 2009 *Phys. Rev. E* **79** 061403
[17] El Shawish S, Dobnikar J and Trizac E 2011 *Phys. Rev. E* **83** 041403
[18] Dobnikar J, Castaneda-Priego R, von Grünberg H H and Trizac E 2006 *New J. Phys.* **8** 277
[19] Earl D J and Deem M W 2005 *Phys. Chem. Chem. Phys.* **7** 3910 and references therein
[20] Wu F Y 1982 *Rev. Mod. Phys.* **54** 235